

## **Recent Progress of NPLS Technique and Its Applications**

### **in Measuring Supersonic Flows**

**YI Shi-he, \*CHEN Zhi, HE Lin, ZHAO Yu-xin, TIAN Li-feng, WU Yu**

College of Aerospace Science and Engineering, National University of Defense Technology, China

\*Corresponding author: gfdchenzhi@163.com

#### **Abstract**

Experimental method is very important and effective to study supersonic turbulence. However, because of the complexity and instability of supersonic turbulence, measuring its fine structures is very difficult for most measurement methods. Nano-tracer planar laser scattering (NPLS) is a new flow visualization technique, which was developed by the authors' group in 2005. It can visualize temporal-resolved flow structure in a cross-section of instantaneous 3D supersonic flow at high spatiotemporal resolution. Many studies have demonstrated that NPLS is a powerful tool to study supersonic turbulence. In recent years, the authors of this paper have made great progresses in supersonic turbulence study using NPLS. And several techniques based on NPLS have been developed by the authors, such as NPLS-based density technique (NPLS-DT), which help us understand the density field of supersonic flows. This paper introduced NPLS technique for visualizing the fine structures of supersonic flows, and reviewed its applications in supersonic mixing layer, supersonic boundary layer, shock/boundary layer interaction, and so on. With its available application on measuring flow static parameters such as Reynold stress and turbulent kinetic energy, NPLS would contributes to the development of turbulence models for compressible flows.

**Keywords: NPLS, supersonic turbulence, fine structure**

#### **0. Introduction**

For the complexity and instability of the supersonic turbulence, measuring its fine structures becomes very difficult. The existing experimental methods have their own shortages for supersonic turbulence study, such as Schlieren, filtered Rayleigh scattering (FRS), and planar laser induced fluorescence (PLIF), and the main reasons are their low resolution and signal noise ratio (SNR) (YI 2009 a). NPLS, as a newly developed flow visualization technique by the authors' group, can visualize temporal-resolved flow structures in a cross-section of instantaneous 3D supersonic flow at high spatiotemporal resolution (ZHAO 2009 a). In recent years, Yi's many studies have demonstrating that NPLS is a powerful tool to study supersonic flow, especially for supersonic turbulence (YI 2009 a – YI 2006 c). In 2007, ZHAO et al visualized the flow structure of pressure unmatched supersonic mixing layer using NPLS, and discussed the influence of shock wave and expand wave on structures of mixing layer and the influence of pressure unmatched (ZHAO 2007 a). Based on NPLS, ZHAO Yu-xin, et al studied the shocklet in supersonic turbulent mixing layer, and in NPLS images the shocklets could be easily distinguished (ZHAO 2007 b). ZHAO et al studied the interaction between shock wave and turbulent mixing layer based on NPLS (ZHAO 2007 c), and observed the interaction between oblique shock wave and boundary layer and the influence of large vortex in mixing layer on oblique shock wave. In 2008, based on NPLS images of supersonic turbulent mixing layer, Yi et al studied the fractal dimension of transition region and turbulence region of supersonic mixing layer. And they found that in the transition region, the

fractal dimension increases with turbulence, and in the turbulence region, the fractal dimension doesn't vary apparently (ZHAO 2008). TIAN et al visualized the supersonic flow around a concave optical spheric conic model by NPLS, and the NPLS images revealed shock wave, expansion wave, turbulent boundary layer and wake in the flow ( TIAN 2009 a). In 2009, Yi et al studied a supersonic mixing layer with convective Mach number at 0.5. From the NPLS image of supersonic mixing layer, we can easily distinguish the fine structures, and estimate its transitional region. Based on the NPLS image, the control effect could be estimated easily (YI 2009 a). And based on the NPLS images, Yi et al analyzed geometrical character and temporal evolution of large-scale structure of turbulent boundary layer. In 2009, Yi Shi-he, et al introduced NPLS technique in detail (ZHAO 2009 a). Nanoparticles are used as NPLS tracer, and pulse planar laser is used as its light source. By recording location of the tracer particles with CCD, the flow structure with high spatiotemporal resolution can be imaged in NPLS image. In literature (ZHAO 2009 a), the flow-following ability and the scattering characteristics of nanoparticles were studied, and the results showed that the dynamic behavior and light scattering characteristics of nanoparticles make NPLS can image the supersonic flow structure at high spatiotemporal resolution and SNR.

Based on NPLS technique, several methods have been developed by the authors. In 2009, TIAN et al developed a density measurement method named NPLS-based density technique (NPLS-DT). This technique can measure planar instantaneous density field in 3D supersonic flow by calibrating the relationship between density field and gray of NPLS image, and has high spatiotemporal resolution (2009 b). In 2010, YI S H, et al proposed an aero-optical aberration measuring method – NPLS-based wavefront technique (NPLS-WT). This method has three significant innovations: (1) high spatiotemporal resolution; (2) it can avoid the integral effects and study the wavefront aberration induced by the flow field of interest locally; (3) it can avoid the influence from the test section wall boundary layers and environmental disturbances (TIAN 2010). Based on NPLS-DT and PIV techniques, measurements on Reynold stress of supersonic turbulence can be realized through special experimental arrangement.

## 1. NPLS Techniques

The authors have studies on measuring the structures of supersonic turbulence by non-intrusive method in recent years, including the traditional interferometry and the optical scattering. The results indicate that because of the influences of compressibility, shock wave, instability, and other factors, the traditional visualization and measurement methods encounter some difficulties. For supersonic flow, the flow visualization technique based on Mie scattering often cannot satisfy the requirement of following the flow faithfully, especially when there are shock waves. On the other hand, for the techniques based on molecule tracer, more expensive intensified CCD is necessary because of its weak signal. Thus, it is difficult to achieve high spatiotemporal resolution for these techniques.

Rapid developments and extensive applications of modern laser technology, imaging, image process technologies, and nanotechnology offer the opportunity for measuring the fine structures of supersonic flow. And in this condition, the authors developed NPLS technique several years ago, which can image fine structures of supersonic flow at high spatiotemporal resolution.

As shown in Fig. 1, the NPLS system is composed of light source system, nanoparticle generator, recording system, synchronization system, and a computer. The light source is a dual-cavity Nd: Yag laser, whose wavelength is 532nm, laser pulse width is 6ns, and pulse energy is 350mJ. A laser sheet with thickness about 0.5mm is formed by the sheet optics system, and then illuminates the flow region of interest. The nanoparticle generator is driven by high pressure, and the concentration

of the output particles can be adjusted. The recording system is an interline transfer CCD whose resolution is  $2048 \times 2048$  and the shortest time interval of double-exposure is  $0.2 \mu\text{s}$ . The synchronizer receive signals sent from the computer, and control the time sequences of laser and the CCD to make sure that the two laser beams are exposed in the frames of dual-exposure respectively. The computer not only sends synchronization signals to the synchronizer, but also stores and processes NPLS images. With the dual-exposure technique, NPLS can measure the instantaneous flow structure, and the temporal evolution of the flow between the two pulses also can be yielded.

The flow-following ability of the NPLS tracer particle in supersonic flow was studied from particle dynamics by ZHAO Y X, et al (ZHAO 2009 a), and the particle diameter was measured with oblique shock wave calibration experiment, as shown in Fig. 2. The effective diameter of nanoparticle of NPLS is  $42.5 \text{ nm}$ , and its relaxation time is  $66.3 \text{ ns}$ . As a flow visualization technique, NPLS focuses on holistic scattering character of a cluster of particles, whose scattering character can be calculated from Mie scattering theory, and the results revealed that its scattering character is relative to scattering angle, wavelength of incident laser, its diameter and refractive index (ZHAO 2009 a).

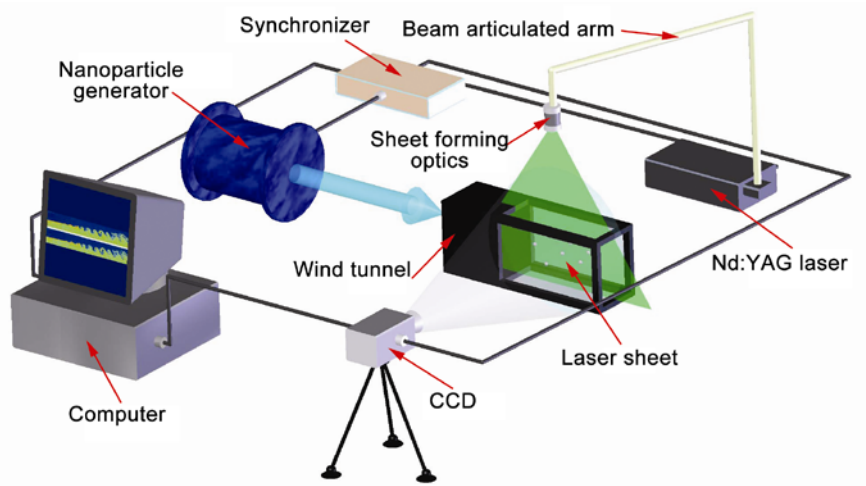
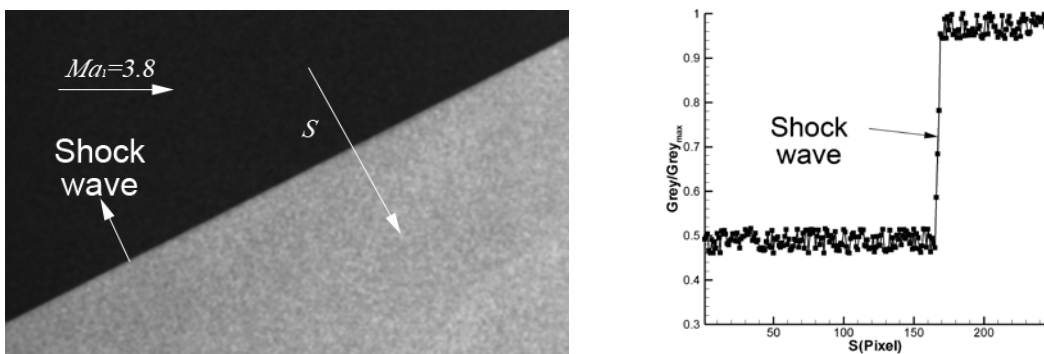


Fig. 1 The sketch of NPLS system



NPLS image of oblique shock wave (b) Relative grey along S  
Fig. 2 NPLS image of shock wave and Relative grey across it

## 2. NPLS application in supersonic flows

For the advantages of NPLS in measuring fine structures of supersonic turbulence, several typical supersonic flows were studied, including supersonic mixing layer and boundary layer, shock/boundary layer interaction and the flow around a spheric conic model.

### 2.1 Supersonic mixing layer

In the past several years, spatiotemporal characteristic of supersonic mixing layers with convective Mach number 0.12, 0.21, 0.24, 0.32, 0.50 and 0.60 were studied by the authors (ZHAO 2008). The supersonic mixing layer wind tunnel is designed using double supersonic laminar nozzle and optical accesses for non-intrusive measurement, which can generate uniform flow filed with low noise, as shown in Fig.3. Changing the Mach number of the double nozzle, various convective Mach number can be gained for experimental study. The results revealed Kelvin-Helmholtz instable vortexes in the flow field. Its spatial features and temporal evolution can be yielded from NPLS images, which are shown in Fig. 4 and Fig. 5. ZHAO et al also studied its spanwise structure, and found the intriguing vortexes due to the secondary instability. Fig. 5 shows Reynold stress of supersonic mixing layer in this plane, which is quite valuable for constructing compressible turbulent models.

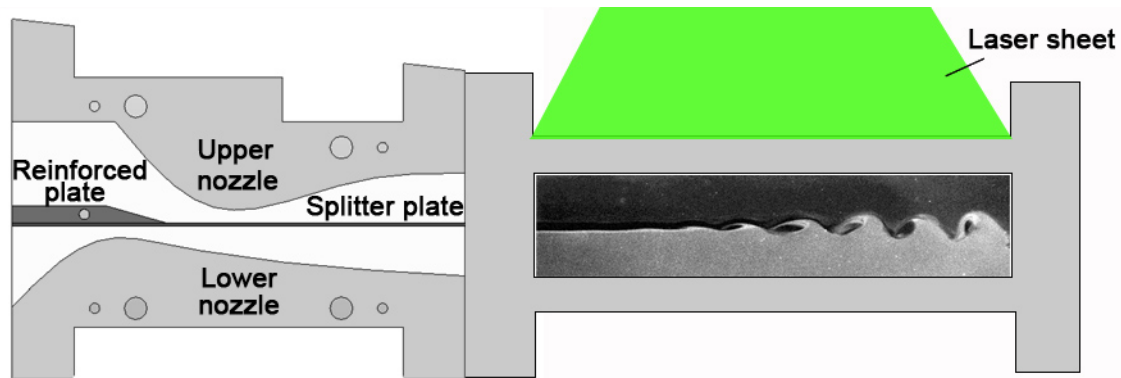


Fig. 3 Nozzle section and test section of the supersonic mixing layer wind tunnel

The NPLS technique has been widely used to study other important problems of supersonic mixing layer, including the velocity field of the transition process (ZHAO 2007 b), the turbulent structure with unmatched pressure (ZHAO 2007 a), the fractal characteristics of the mixing interface (ZHAO 2008), and the multiresolution analysis of the density field (ZHAO 2010).

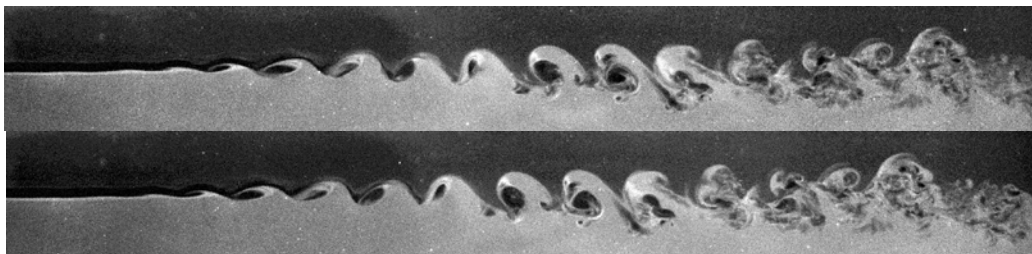


Fig. 4 NPLS images of K-H vortexes of supersonic mixing layer

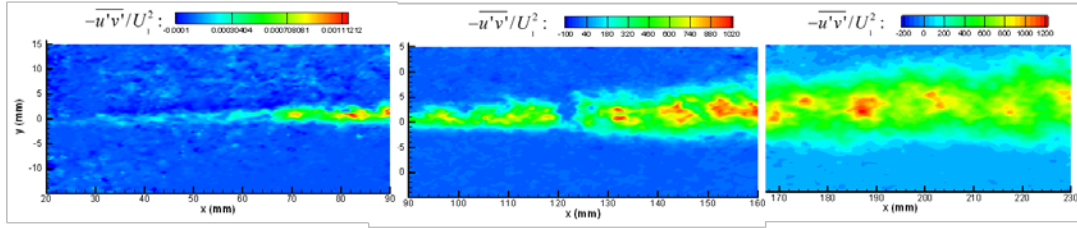


Fig. 5 Reynolds stress of supersonic mixing layer based on NPLS

## 2.2 Flow around a spheric conic model

The flow field around a spheric conic model in  $Ma=3.8$  flow was studied using NPLS, and its flow structure (TIAN 2009 a), density field (TIAN 2009 b), velocity field (TIAN 2010), and aero-optical effect (YI 2010) were studied. The structure of the flow around a spheric conic model is rather complex, which includes shock wave, expansion wave, boundary layer and wake. As shown in Fig. 6 are NPLS image of the flow field and the corresponding density field measured by NPLS\_DT. Compared with the results obtained by schlieren, the shock waves in NPLS image is much thinner. The reason is that the spatial resolution of the NPLS is much higher than that of schlieren. The density field in Fig.6 shows clearly the existence of flow structures mentioned above, and the transition of boundary layer.

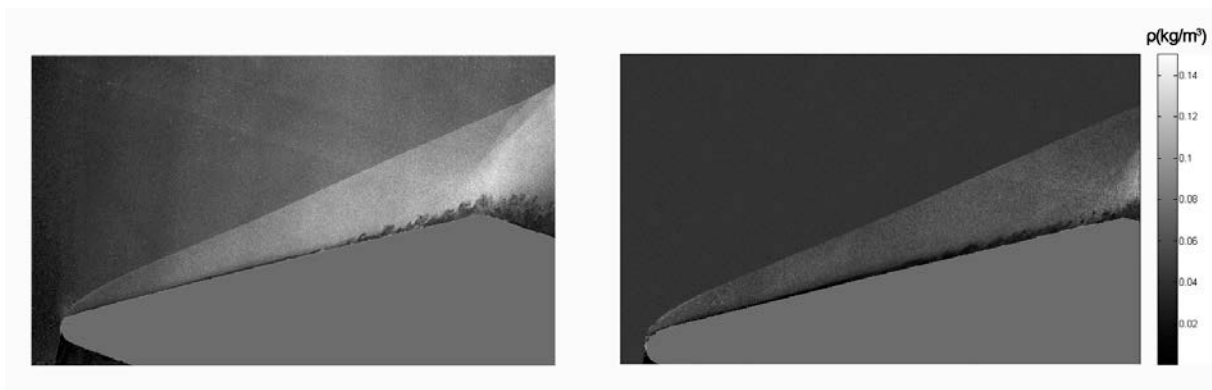


Fig. 6 NPLS image and corresponding density field of the flow around a spheric conic model in  $Ma=3.8$  flow

## 2.3 Supersonic boundary layer

Supersonic boundary layer, another typical flow, has been studying using NPLS in the past several years. The flow structure of the supersonic boundary layer in vertical plane and spanwise plane were captured by NPLS.

As shown in Fig. 7 is a NPLS image of flat plate boundary layer in vertical plane in  $Ma=3$  flow, and the flow region is 100-320mm from the leading edge of plate. Fig. 7 displays the whole transition process of the boundary layer. Until 180mm distant from the leading edge, the flow is still laminar. Then follows transition, and flow becomes fully developed from  $X=250$ mm. Fig. 8 and Fig. 9 are the flow regions within 170-250mm and 190-220mm from the leading edge of the plate, respectively. From these images, it is easy to find the development of instability and the emergence of hairpin vortexes. Fig. 10 is the NPLS image of fully developed turbulent boundary layer, whose flow region is 250-320mm from the leading edge. Compared with the cases in Fig. 8 Fig. 9, the flow structures in Fig. 10 are different absolutely and much more complex. However, the fine structures in the turbulent boundary layer were revealed clearly in Fig. 10 all the same. Fig. 11 (left)

shows the Spanwise NPLS image of supersonic boundary layer corresponding to Fig. 6. And in addition, the fully developed turbulent boundary layer of wind tunnel is different from that on a flat plate, as shown in Fig. 11 (right). By performing PIV technique, time-averaged streamwise velocity profiles at different locations and Reynolds stress distributions of turbulent boundary layer are present as shown in Fig. 12 to Fig. 14.

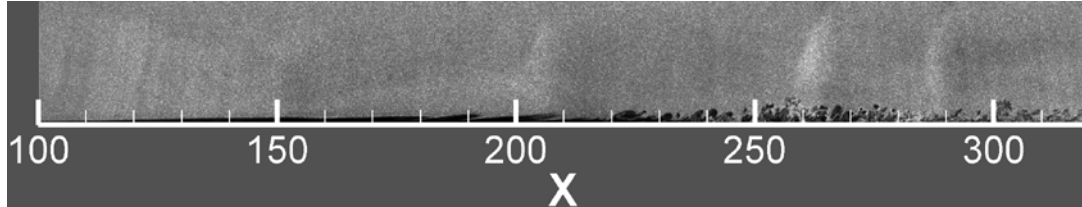


Fig. 7 NPLS image of supersonic boundary layer in Ma=3 flow

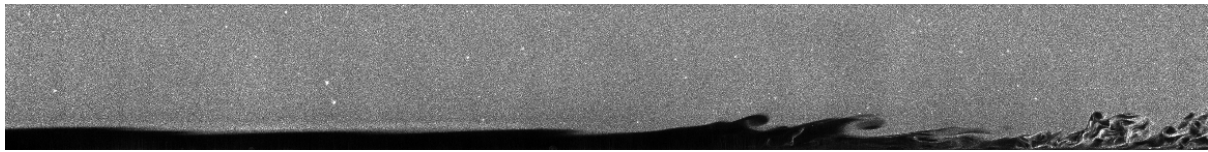


Fig. 8 NPLS image of supersonic boundary layer in the front of the plate

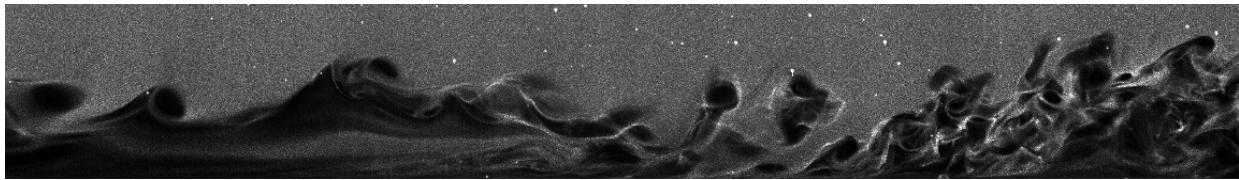


Fig. 9 NPLS image of supersonic boundary layer in the middle of the plate

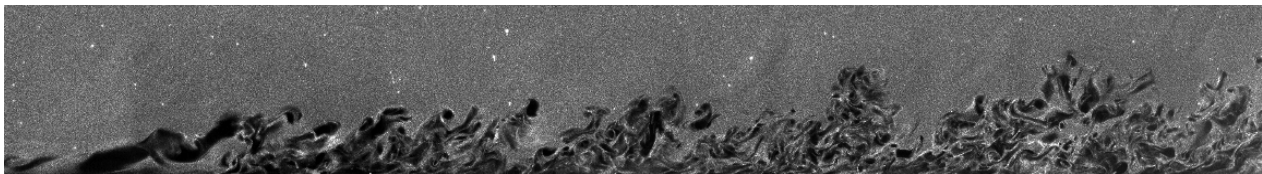


Fig. 10 NPLS image of fully developed supersonic turbulent boundary layer

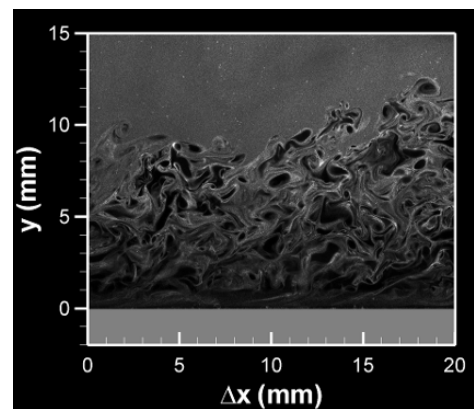
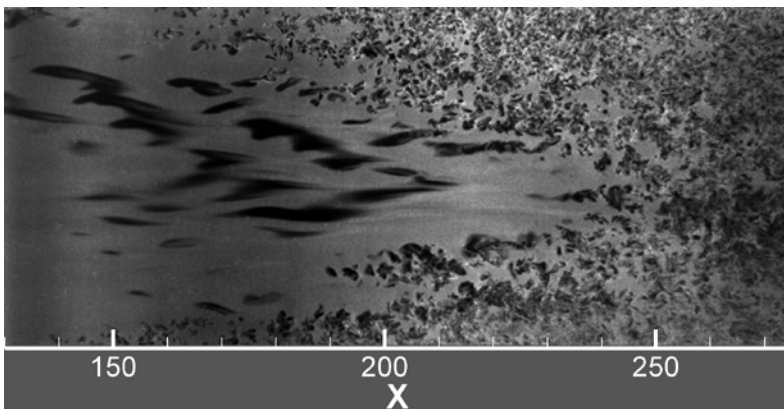


Fig. 11 Spanwise NPLS image of supersonic boundary layer in Ma=3 flow (left) and the fully developed supersonic turbulent boundary layer of wind tunnel (right)

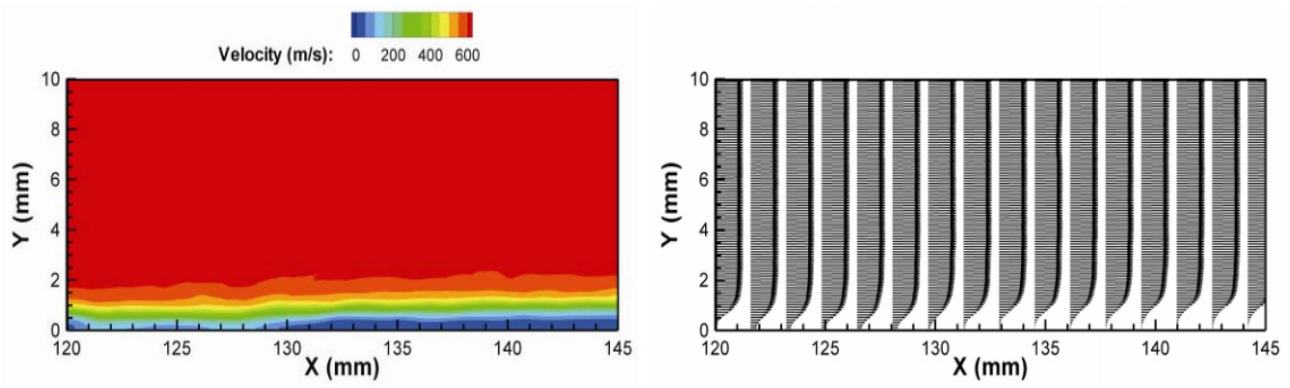


Fig. 12 Time-averaged velocity of supersonic boundary layer in the front of the plate corresponding to Fig.8

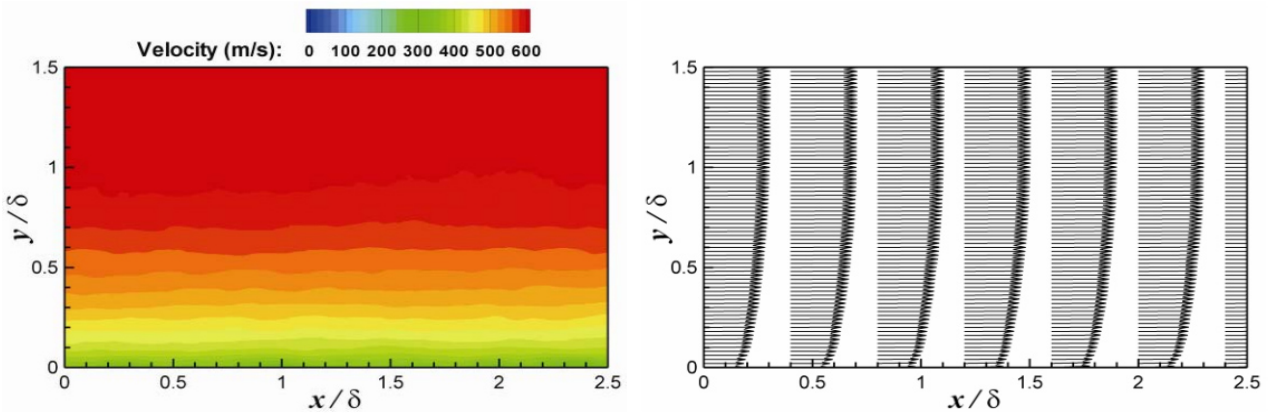


Fig. 13 Time-averaged velocity of fully developed supersonic turbulent boundary layer corresponding to Fig.10

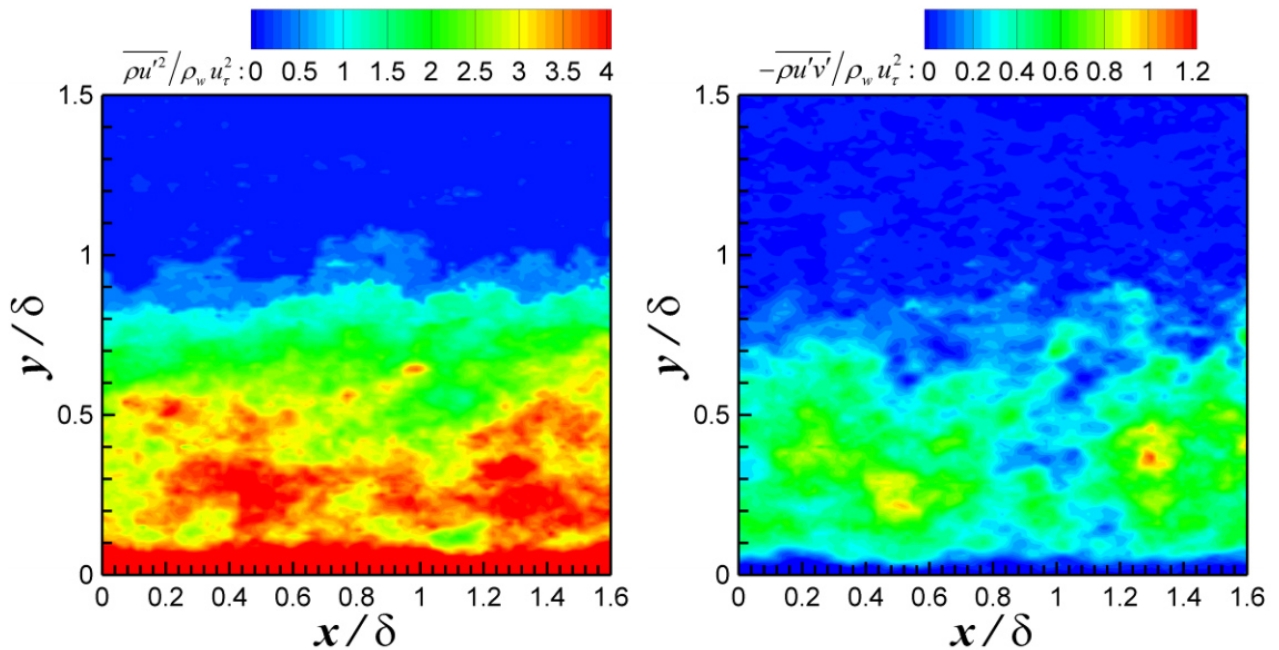


Fig. 14 Reynolds stress distribution of fully developed supersonic turbulent boundary layer corresponding to Fig.11 (right)

## 2.4 Shock/boundary layer interaction

Based on NPLS, the structure of shock/boundary layer interaction (SWBLI) was studied in this paper. As shown in Fig. 15 is the NPLS image of SWBLI in  $Ma=3$  flow, and its spatial resolution is  $43.5\mu\text{m}/\text{pixel}$ . The image revealed shock wave, expansion wave, turbulent boundary layer, and separation bubble. From the NPLS image, we can find that the vortex moves downstream, and its transfiguration is not obvious. Using NPLS\_DT, the density field of the flow field shown in Fig. 15 was measured at high spatial resolution. Density variation and temporal evolution of the SWBLI can be distinguished easily. Fig. 16 is the velocity field and the stream lines of the SWBLI flow field.

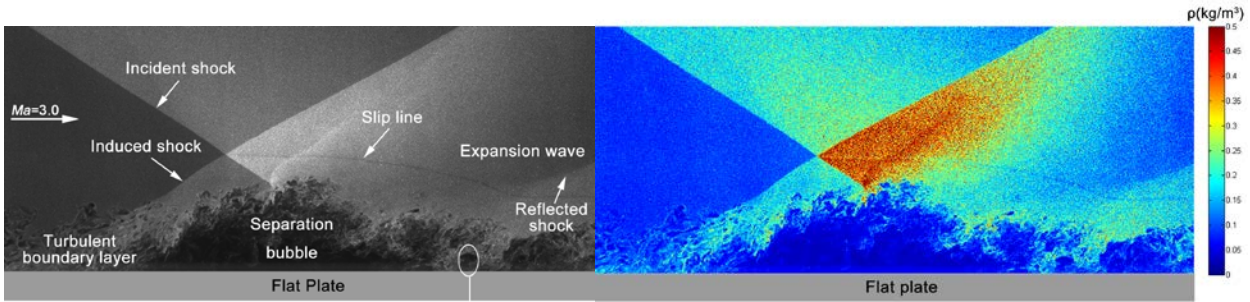


Fig. 15 NPLS image and the corresponding density field of shock/boundary layer interaction in  $Ma=3$  flow

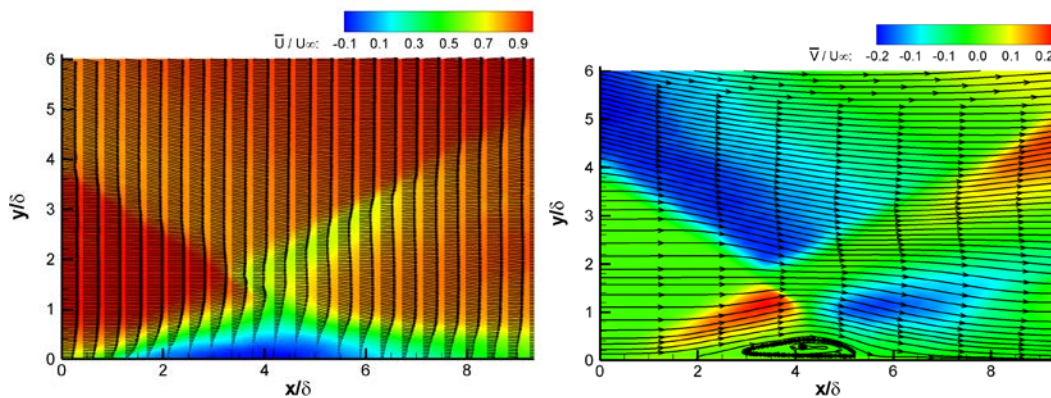


Fig. 16 Velocity field and the corresponding stream lines of the flow field as shown in 11

## 2.5 Supersonic Flow over a Compression Ramp

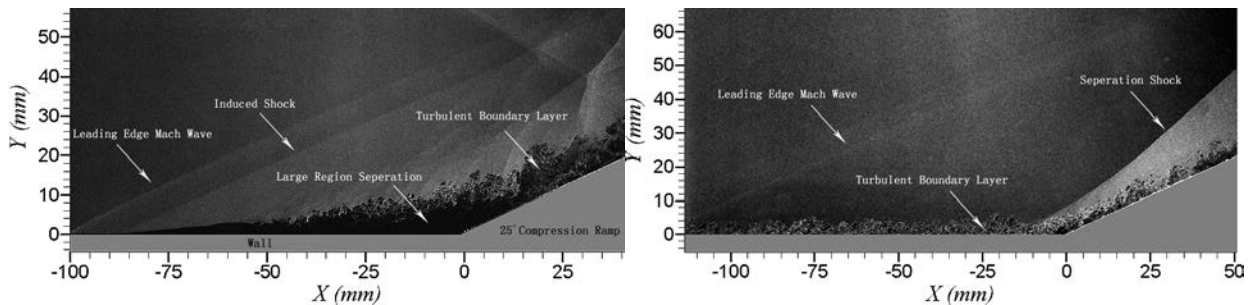


Fig. 17 Supersonic laminar flow (left) and supersonic turbulent flow (right) over a compression ramp

NPLS images of supersonic laminar/turbulent flow over a compression ramp are shown in Fig. 17, it can be seen distinctly from the images that there are obvious differences between the laminar flow

and the turbulent flow in compression ramp, even though the ramp angle is the same. For laminar flow, the development of the supersonic flow and its transition to turbulence are rapid. Flow separation occurs with the influence of adverse pressure gradient. Some typical flow structures such as K-H vortices, shear layer, separation shock and reattachment shock are visible clearly. However the thickness of turbulent boundary layer does not increase obviously and there is not evident separation in the flow field, as shown in Fig. 17 (right). The boundary layer adheres to the wall in the whole flow field. These experimental results of flow visualization have revealed that, compared with laminar flow, the performance of turbulent flow is more stable when suffering the effects of adverse pressure gradient, and is more difficult to separate.

### 3. Conclusions

From the results mentioned above, we can find that NPLS is a powerful tool to visualize the fine structures of supersonic turbulence and measure the corresponding instantaneous density and velocity field. A great number of experiments have been performed, and several important flow structures have been revealed by NPLS images. As a newly developed technique, however, NPLS and its application are still under development.

Currently, the measurement region of NPLS is only the scattering plane of laser pulse, and the temporal-resolved images are restricted to the pair obtained by frame, which prevents it from giving a more complete description of the flow structure. We are now updating the crucial components of the system to overcome these limitations, including employing multi-cavity laser to achieve high repetition frequency (hundreds of millions per second), employing proper CCD with very high recording speed and the synchronizer with accuracy of picosecond. Our ultimate goal is to synchronously measure several parameters (including density, velocity) of super flow with temporal correlation across many frames.

### Acknowledgement

The project is supported by National Basic Research Program of China (Grant NO. 2009 CB724100), National Natural Science Foundation of China (Grant NO. 11172326), innovation fund program for outstanding postgraduate students of NUDT (Grant NO. B120103) and Hunan Provincial Innovation Foundation for Postgraduate (CX2012B002).

### References

- YI S H, HE L and ZHAO Y X. (2009 a), A flow control study of a supersonic mixing layer via NPLS. *Sci China Ser G*, 2009, 52(12): 2001-2006.
- ZHAO Y X, YI S H, TIAN L F. (2009 a), Supersonic Flow imaging via nanoparticles. *Science China Ser E- Tech Sci*, 2009, 52(12): 3640-3648.
- ZHAO Y X, YI S H, TIAN L F. (2009 b), The quantificational measurement of supersonic mixing layer growth rate. *Journal of experiments in Fluid Mechanics*, 2009, 23(3): 100-103.
- YI S H, ZHAO Y X, TIAN L F. (2009 a), Recent advances of experimental study of supersonic mixing layer transition. *ACTA AERODYNAMICA SINICA*, 2009, 27: 114-119.
- TIAN L F, YI S H, ZHAO Y X. (2009 a) Flow visualization of supersonic flow around a concave optical bow cap model. *Journal of experiments in Fluid Mechanics*, 2009, 23(1): 15-17.
- ZHAO Y X, TIAN L F, YI S H. (2007 a) Experimental study of flow structure in pressure unmatched mixing layer [J]. *Journal of experiments in Fluid Mechanics*, 2007, 21(3): 14-17.
- ZHAO Y X, YI S H, HE L. (2007 b), The experimental research of shocklet in supersonic turbulent mix layer. *Journal of National University of Defense Technology*, 2007, 29(1): 12-15.
- ZHAO Y X, YI S H, HE L. (2007 c), The experimental study of interaction between shock wave and turbulence. *Chinese Science Bulletin*, 2007, 52(10): 1297-1301.
- ZHAO Y X, YI S H, HE L. (2008), The fractal measurement of experimental images of supersonic turbulent mixing layer. *Sci China Ser G-Phys Mech Astron*, 2008, 51(8): 1134-1143.

- ZHAO Y X. (2008), Experimental investigation of spatiotemporal structures of supersonic mixing layer. PhD Thesis, National University of Defense.
- YI S H, ZHAO Y X, TIAN L F. (2008), Advances of experimental study to transition of supersonic mixing layer. Proceedings of the 13th national symposium on shock wave and shock tube technology, ChangSha.
- YI S H, ZHAO Y X, HE L. (2006 a), Experimental study of temporal and spatial characters of the transition of supersonic mixing layer. Proceedings of the 12th national symposium on shock wave and shock tube technology, LuoYang.
- YI S H, ZHAO Y X, HE L. (2006 b), Fractal study of experiment images of supersonic mixing layer. Proceedings of the 12th national symposium on shock wave and shock tube technology, LuoYang.
- YI S H, ZHAO Y X, HE L. (2006 c), The quantificational measurement of supersonic mixing layer growth rate based on NPLS image. Proceedings of the 12th national symposium on shock wave and shock tube technology, LuoYang.
- ZHAO Y X, Yi S H, TIAN L F. (2009), An experimental study of aero-optical aberration and dithering of supersonic mixing layer via BOS. SCIENCE CHINA: Physics, Mechanics & Astronomy, 2009, 53(1): 81-93.
- TIAN L F, YI S H, ZHAO Y X. (2009 b), Study of density field measurement based on NPLS technique in supersonic flow. Sci China Ser G, 2009, 52(9):1357-1363.
- ZHAO Y X, YI S H, TIAN L F. (2010), Multiresolution analysis of density fluctuation in supersonic mixing layer. Sci China Tech Sci, 2010, 53(2): 584-591.
- YI S H, TIAN L F, ZHAO Y X. (2010), Aero-optical aberration measuring method based on NPLS and its application. Chinese Sci Bull, 2010, 55(31): 3545-3549.
- TIAN L F, YI S H, ZHAO Y X. (2010), PIV study of supersonic flow around an optical bow cap. Journal of experiments in Fluid Mechanics, 2010, 24(1): 26-29.
- ZHANG M L, YI S H, ZHAO Y X. (2007), The design and experimental investigations of supersonic length-shortened nozzle. ACTA AERODYNAMICA SINICA, 2007, 25(4): 500-503.
- HE L, YI S H, ZHAO Y X. (2010), The application of BOS in flow measurement. Journal of National University of Defense Technology, 2010, 31(1): 1-5.